Electronic Supplementary Information

Integrating DNA Strand Displacement Circuitry to Nonlinear Hybridization Chain Reaction

Zhuo Zhang, [a] Tsz Wing Fan [b] and I-Ming Hsing *[a, b]

a, Division of Biomedical Engineering, The Hong Kong University of Science and Technology
b, Department of Chemical and Biomolecular Engineering, The Hong Kong University of Science and Technology, Clear Water Bay, Kowloon, Hong Kong

*Email: kehsing@ust.hk

The file contains:

a) Section 1: Sequence Design
b) Section 2: Supplemented PAGE and real-time fluorescence results
c) Section 3: Design strategy to reduce downstream leakage
d) Section 4: Fold amplification comparison of upstream, downstream and integrated amplifiers

Section 1. Sequence Design

The sequences used in this work were designed to have minimally spurious interactions. DNA strands interactions were predicted and examined using Nupack[1-3]. Extra efforts were applied to ensure that single-stranded reactants and products possessed no significant secondary structure, e.g. the upstream F strand, O strand and downstream assistants, since significant secondary structure would slow the rates of hybridization and branch migration[4]. 2nt clamping segments were attached at each blunt end of the multi-stranded substrates, aiming to reduce the effect of "breathing" phenomenon on the unintentional crosstalks. 20 bases poly-T tail was added to the 5' end of O strand, in order to differentiate its band in the PAGE gel.

Table S1. DNA sequences

Upstream (8nt/5nt) for **Mir 21**	Trigger (Mir 21)	5'-TAGCTTATCAGACTGATGTTGA-3'
	Bottom-S strand(Mir 21)	5'-TCAACATCAGTCTGATAAGCTATAAGGGAGATGTGA GAGGAAGAAGGATAAGAG-3'
	By-product 1(Mir 21)	5'-CCTTATAGCTTATCAGACT-3'
	Fuel (Mir 21)	5'-CCTTCTTCCTCTCACATCTCCCTTATAGCTTATCAGACT-3'
for **miR-150**	Trigger(miR-150)	5'-TCTCCCAACCCTTGTACCAGTG-3'
	Bottom-S strand(miR-150)	5'-CACTGGTACAAGGGTTGGGAGATAAGGGAGATGT GAGAGGAAGAAGGATAAGAG-3'
	By-product 1(miR-150)	5'-CCTTATCTCCCAACCCTTG-3'
	Fuel (miR-150)	5'-CCTTCTTCCTCTCACATCTCCCTTATCTCCCAACCCTTG-3'
for **miR-200a**	Trigger(miR-200a)	5'-TAACACTGTCTGGTAACGATGT-3'
	Bottom-S strand(miR-200a)	5'-ACATCGTTACCAGACAGTGTTATAAGGGAGATGTGAG AGGAAGAAGGATAAGAG-3'
	By-product 1(miR-200a)	5'-CCTTATAACACTGTCTGGT-3'
	Fuel (miR-200a)	5'- CCTTCTTCCTCTCACATCTCCCTTATAACACTGTCTGGT-3'
Universal upstream strands	Output strand	5'-TTTTTTTTTTTTTTTTTTTTCTCTTATCCTTCTTCCTCTCACATCTC-3'
	Reporter F strand	5'-/5Alex647N/GTGAGATGTGAGAGGAAGAAGGATAAGAG-3'
	Reporter Q strand	5'-CCTTCTTCCTCTCACATCTCAC/3IAbRQSp/-3'
Universal Downstream	F-strand of SA	5'-/56-FAM/GACCCATAAACTAAACTCACTTGGACCCATAAACTAA ACTCACTTGGATGTGAGAGGAAGAAGGATAAG-3'
	Q-strand of SA	5'-CCTTCTTCCTCTCACATCGTTTAGTTTATGGGTCGTTTAGTTTATG GGTC/3IABkFQ/-3'
	F-strand of SB	5'-CAAGTGAGTTTAGTTTATGGGTCCTTATCCTTCTTCCTCTCACATC CTTATCCTTCTTCCTCTCACATC/36-FAM/-3'
	Q-strand of SB	5'-/5IABkFQ/GATGTGAGAGGAAGAAGATGTGAGAGGAAGAAGAC CCATAAACTAAACTC-3'
	Assistant AA	5'-CCCATAAACTAAACGACCCATAAACTAAACGATGTG-3'
	Assistant BB	5'-TGGGTCTTCTTCCTCTCACATCTTCTTCCTCTCACA-3'

The underlined characters denote the toeholds.

Section 2. Supplemented PAGE and real-time fluorescence results.

Fig. S1 Non-denaturing PAGE analysis examined the effects of lengths and ratios of the exposed toehold (domain 6) and the hidden toehold (domain 4) in substrate S on the upstream process.

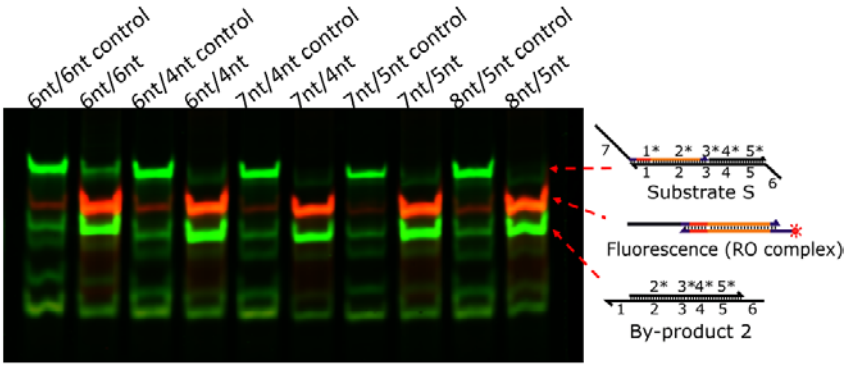

Figure S1. PAGE (12% gel) analysis of the effect of toehold lengths (domain 6 vs. domain 4) on the yield of Output strand (O strand). Five scenarios of toehold lengths were tested, which are indicated on the top of each gel lane. E.g. 7nt/4nt means the toeholds length of domain 6 and domain 4 being 7nt and 4nt, respectively. Red-color fluorescent bands represent the RO complex formed when O strand released from upstream reacted with the reporter duplex. [S] = 0.6μM, [F] = 1.5μM, [R] = 0.6μM, [T] = 0.3μM (Mir 21), mixed and incubated at room temperature for 1 hour.

Fig. S2 Downstream system leakage with original assistant design.

For downstream only kinetics measurement (Fig. S2 (a)), since the lowest target concentration tested is 0.001x (0.1nM), the end-point signal of 0.001x data was set as 100n.u. and other traces were normalized accordingly. As shown in Fig.S2 (a), even in the absence of O strand, SA and SB could initiate the hyperbranched growth autonomously when assistant strands AA and BB are present in the mixture. A part of the fluorescence signal observed for 0x trigger is caused by a few imperfectly annealed SA and SB, and the rest is contributed from the systematic leakage of the original downstream design. Fig S2 (b) reveals the linear fit of the plot of the time required to achieve a normalized fluorescence intensity of 100 n.u. against the logarithm of the concentration of O strand added.

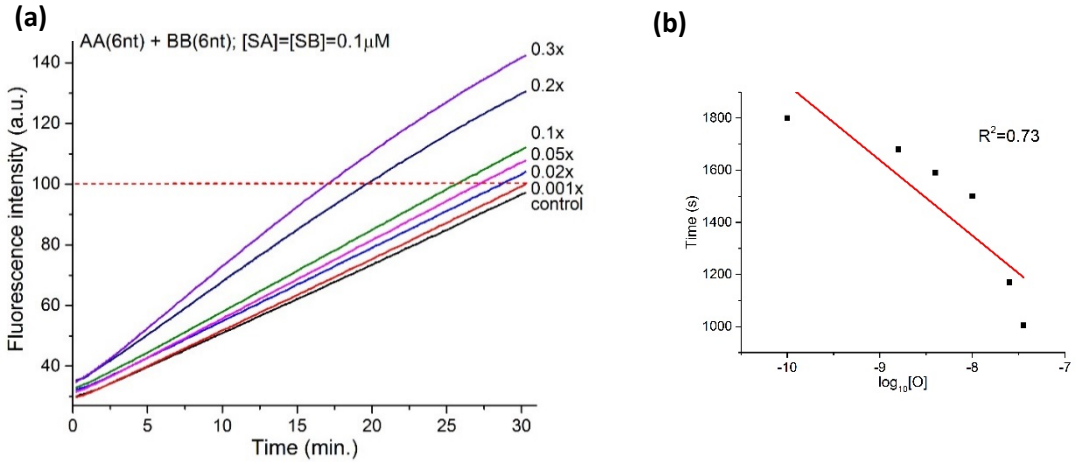

Figure S2. (a) Real-time fluorescence measurement of downstream subsystem with original assistant design. 0.001x trigger means the concentration of O strand is 0.001 times the concentration of SA. (b) The linear fit of the plot of the time required to achieve a normalized fluorescence intensity of 100 a.u. against the logarithm of the concentration of O strand added. R^2=0.73.

Fig. S3 Integrated system leakage with original assistant design.

Whereas for integrated circuitry monitoring (Fig.S3 (a)), as the lowest input concentration tested is 0.0005x (0.05nM), the end-point signal of 0.0005x data was set as 50 n.u. and corresponding fluorescent data normalization was conducted. Similarly, as indicated in Fig. S3(a), in the absence of Mir21 target which leads to the release of O strand, the downstream SA and SB could initiate the hyperbranched growth spontaneously at the present of assistant strands AA and BB. A part of the fluorescence gain observed for control (un-triggered) is cause by a few imperfectly annealed SA and SB, and the rest is contributed from the downstream system leakage as shown in Fig. S2 (a).

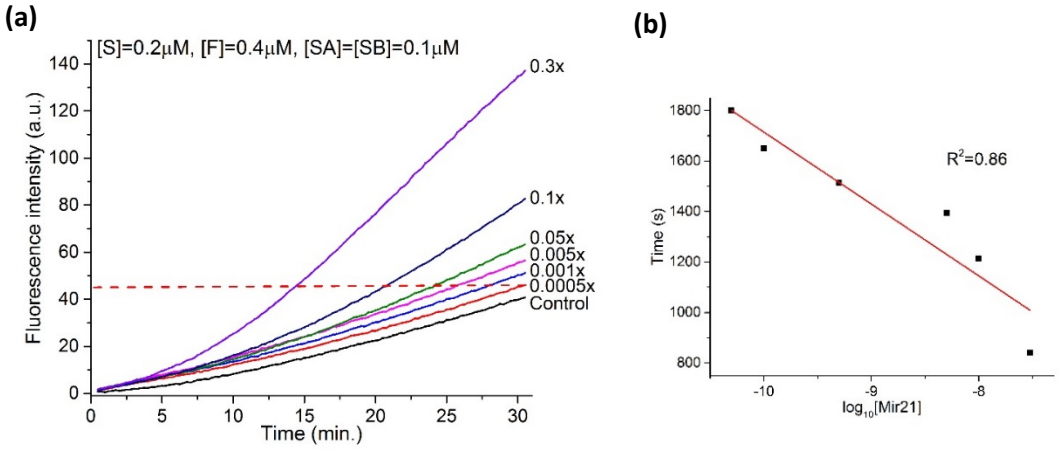

Figure S3. (a) Real-time fluorescence measurement of integrated system with original assistant design. 0.0005x trigger means the concentration of Mir21 is 0.0005 times that of SA. (b) The linear fit of the plot of the time required to achieve a normalized fluorescence intensity of 45 a.u. against the logarithm of the concentration of Mir21 added. R^2=0.86.

Section 3. Design strategy to reduce downstream leakage

In our strategy, target trigger recycling and production of the coupling output O strand are to be executed by the upstream circuit. The objective of the downstream circuit is, on the other hand, to achieve signal amplification through rapid assembly of hyperbranched DNA products. Any tiny leakage in the downstream could unavoidably be amplified, leading to noticeable noises and lower sensitivity of the integrated system.

The reaction leakage, in the downstream, originates from the aberrant interactions between the assistant strands (AA and BB) and substrate SA and SB strands. As part of the self-assembly strategy, there would be regions in SA complementary to AA and in SB complementary to BB strands (Table S1). Although the hybridization reactions among them were not supposed to occur without the presence of output strand O, nevertheless, it could happen because of the breathing and fraying behavior of DNA structure[5-7]. The transient opening due to breathing at the blunt ends near the bulge loops on SA and SB strands unwinds the duplex, lower the energy barrier for the assistant strands to attack. One possible strategy to address this leakage issue is to introduce a mismatch hotspot between the complementary region in the pairs of SA/AA strands and SB/BB strands, a strategy that was reported by other groups.[8-10]

In particular, the study by Turberfield and co-workers[10, 11] has revealed that the kinetics of DNA strand displacement can be tuned up by three orders of magnitude without affecting the reaction free energy, by introducing a proximal mismatch adjacent to the invading toehold. Hence, in our strategy, both assistant strands AA and BB have been devised with a single-base mismatch at position near their corresponding toehold (i.e. 6th or 7th

base counting from 3’ end of AA and 5’ end of BB). The detailed designs of the mismatched-assistant strands are given in Table. S2.

Table S2. DNA sequences for revised assistant designs

Mismatched	AA m6C	5’- CCCATAAACTAAACGACCCATAAACTAAACCATGTG-3’
	AA m6C + 1nt	5’- CCCATAAACTAAACGACCCATAAACTAAACCATGTGA-3’
	AA m7G	5’- CCCATAAACTAAACGACCCATAAACTAAAGGATGTG-3’
	AA m7G + 1nt	5’- CCCATAAACTAAACGACCCATAAACTAAAGGATGTGA-3’
	AA m7G + 2nt	5’- CCCATAAACTAAACGACCCATAAACTAAAGGATGTGAG-3’
	BB m6A	5’- TGGGTATTCTTCCTCTCACATCTTCTTCCTCTCACA-3’
	BB m6A + 1nt	5’- ATGGGTATTCTTCCTCTCACATCTTCTTCCTCTCACA-3’
	BB m6A + 2nt	5’- TATGGGTATTCTTCCTCTCACATCTTCTTCCTCTCACA-3’
	BB m6A + 3nt	5’- TTATGGGTATTCTTCCTCTCACATCTTCTTCCTCTCACA-3’
	BB m7A	5’- TGGGTCATCTTCCTCTCACATCTTCTTCCTCTCACA-3’
	BB m7A + 1nt	5’-ATGGGTCATCTTCCTCTCACATCTTCTTCCTCTCACA-3’
Shortened	AA-4nt	5’-CCCATAAACTAAACGACCCATAAACTAAACGATG-3’
	AA-3nt	5’-CCCATAAACTAAACGACCCATAAACTAAACGAT-3’
	BB-4nt	5’-GGTCTTCTTCCTCTCACATCTTCTTCCTCTCACA-3’
	BB-3nt	5’-GTCTTCTTCCTCTCACATCTTCTTCCTCTCACA-3’

The underlined characters denote the toeholds. Red color marks the mutated base, and purple marks the prolonged bases. The design rule of single-base mutation depends on the ddG and secondary structure change before and after revision, such that the introduced mismatch would not significantly affect the free-energy change nor introduce significant secondary structure to impede the reaction process. The secondary structure was predicted using Nupack and the ddG calculation was based on “mismatch destabilizing bubbles” and examined using matlab.

Non-denaturing PAGE analysis of the downstream process with distinct mismatch-modified assistant strands is shown in Fig. S4 (a). The consumption of substrate bands in control lanes clearly indicates the system leakage. As shown, compared to group ⓪(AA+BB), in the absence of O strand, substrate bands were much less used and assembly products with high molecular weights were effectively diminished when AA and BB were both single-base mutated, either for 1.5 hrs or even 24 hrs assay time, suggesting that the mismatch strategy is successful in minimizing the leakage.

However, even with O strand’s presence, much reduced amounts of hyperbranched products were observed in mutated assistant strand groups than the original design, particularly for short assay time (1.5hrs). This suggests that although the unintentional leakage was reduced, the mismatch strategy also raised the kinetic barrier between exposed SA and SB strands and the assistant strands containing a mismatch site. This slow kinetics of the assembly process could be improved by elongating the toeholds length in assistant strands with a few bases (Table. S2, Fig. S4 and S5) so that the toehold initiation step gets more stabilized and the toehold is less likely to spontaneously detach before branch migration proceeds.[10] As evident by the PAGE result, the kinetics was enhanced when mutated strand’s toehold was prolonged with one more base (i.e. compare the assembled hyperbranched products of group ② and ④ with group ① and ③, respectively). Fig. S4 (b) shows how the kinetics of downstream leakage depends on the position of and the toehold length before a single mismatch introduction on AA and BB strands.

The leakage reaction kinetics was very sensitive to single-base mutations in the assistant strands. Three different kinetic regimes were observed: a high-rate regime for no mismatches, indicating relatively high leakage for original design; a low-rate regime for mutations in both strands, in spite of few bases toehold elongation; and a region in between in which only AA or BB strand was introduced with a single-base mismatch. Although the mismatch approach seems to work in some scenarios, the design strategy is not flexible and the position of mismatch point needs to be experimentally optimized.

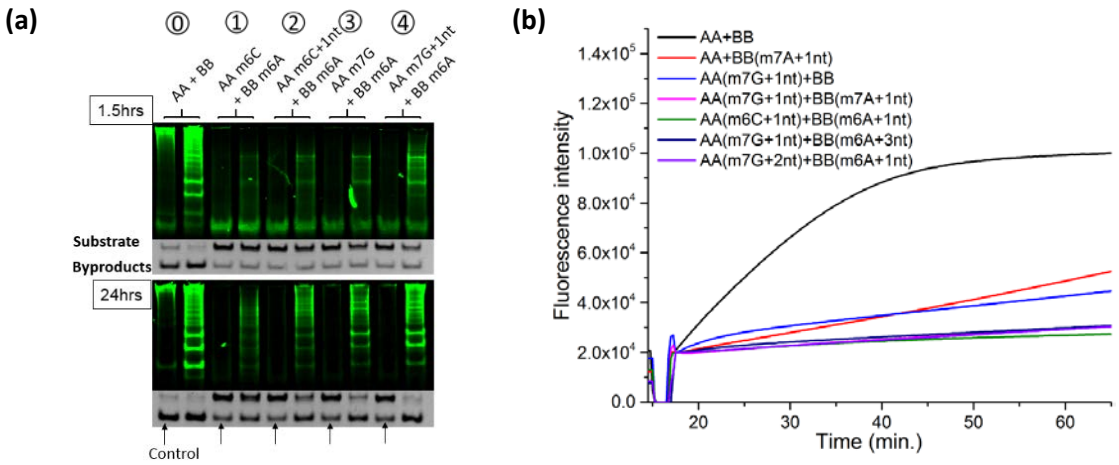

Figure S4. Characterizations of downstream subsystem adopted with mismatch strategy. (a) PAGE (8% gel) analysis examined the effects of mismatch position and toehold lengths in assistant strands on downstream dendrimer self-assembly. Four distinct groups were tested (groups ①, ②, ③, ④) and compared to our original design (group ⓪). The label "m" represents mismatch and '+1nt' means 1nt base toehold elongation. E.g. 'AA m6C + 1nt' means the 6th base counting from AA toehold end (3' end) was mutated to base C, and the toehold length was prolonged with 1 more base. Each group consisted of a control experiment (marked with arrow) and a positive experiment (the lane next to control). Green-color fluorescent bands represent the hyperbranched products assembled by downstream SA and SB. Grey bands indicated the resumed substrates and production of byproducts after reaction. [SA] = [SB] = 0.15μM, [O] = [SA] for positive experiments. Both 1.5hrs and 24hrs timescale were applied to the experiments and compared in the gel. (b) Real-time kinetics measurement evaluated the system leakage for revised downstream self-assembly. Seven groups were tested including four groups with both AA and BB modified with distinct mismatch positions and toeholds elongation, two groups with only AA or BB mutation and one group with original AA and BB design for comparison. No O strand was added, [SA] = [SB] = 0.15μM.

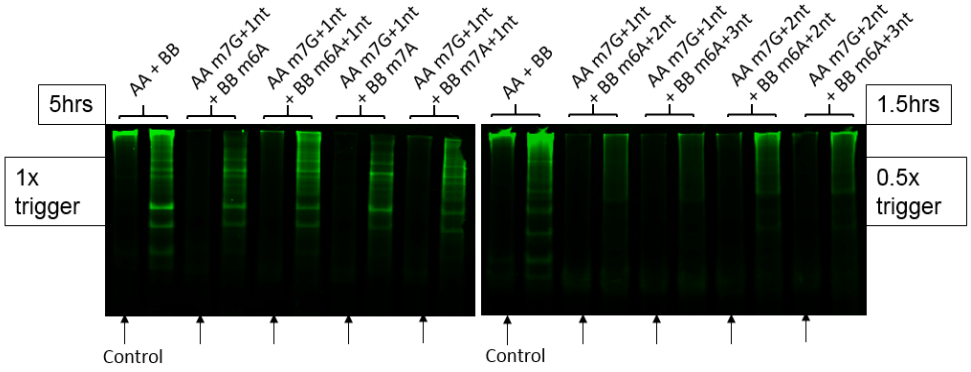

Figure S4. PAGE (8%) analysis evaluated the revised downstream reaction. The label "m" represents mismatch and '+2nt' means 2nt base toehold elongation. E.g. 'BB m6A + 2nt' means the 6th base counting from BB toehold end (5' end) was mutated to base A, and the toehold length was prolonged with 2 more base, i.e. in total 7nt toehold length, with 8th base mutation. Each group consisted of a control experiment (marked with arrow) and a positive experiment (the lane next to control). Green-color fluorescent bands represent the hyperbranched products assembled by downstream SA and SB. [SA] = [SB] = 0.15μM. For left panel, 1xtrigger (O strand) was added as positive control, meaning that the concentration of O strand added is equal to the concentration of SA. The reaction was conducted at room temperature for 5 hrs. For right panel, 0.5xtrigger was added as positive control, meaning that the concentration of O strand added is 0.5 times the concentration of SA. The reaction was performed at room temperature for 1.5 hrs.

An alternative approach to minimize the leakage is to tailor the invading toehold lengths (e.g., from 6 nt down to 4nt or 3 nt) in the assistant strands. Obviously, the shorter the invading toehold, the higher the kinetic barrier[9, 12] of the underlying assembly reaction. Although the shortening of the toehold would reduce the rate of both intentional

and unintentional (leakage) assembly, the reaction triggered by the output O strand should prevail and accelerate at a much higher rate than that of the leakage interaction.

Similarly, non-denaturing PAGE analysis was carried out for detailed characterizations (Fig. S6 (a)). Specifically, four scenarios of shorter toehold were examined and compared to the original design, i.e. AA and BB strands with 6nt length toeholds. As expected, the leakage was greatly suppressed when AA or BB was shortened, given their much less consumption of substrate bands in control lanes. Interestingly, for group ④ (AA-4nt + BB) in Fig. S6 (a), the leakage was significant compared to other shortened assistant groups. This can be ascribed to the major leakage contribution from the reaction between BB and QB, thus when BB was not shortened and AA maintained 4nt toehold domain, which length remains supportive to initiate the branch migration and this combination consequently barely reduced the previous leakage. Hereto, we chose AA and BB both shortened to 4nt toeholds to achieve the trade-off between controlled leakage and sufficient reactivity. Diverse O strand concentrations were added to quantitatively evaluate the growth kinetics via PAGE analysis and real-time fluorescence measurement. As anticipated, when assistant strand toeholds were shortened, the overall kinetics of hyperbranched self-assembly was consistently depressed (Fig. S6 (b)). It is noted that when AA and BB were devised to 4nt toeholds, the downstream sub-system exhibited an improved discriminating ability compared to the former system (Fig. 3(b)), especially in low concentration regime (Fig. S6 (c)), although longer assay time is required to compensate the impeded kinetics. This result indicated that the shorten toeholds strategy may be a worth-trying approach to regulate the kinetics of the dynamic hyperbranched growth with well-controlled leakage.

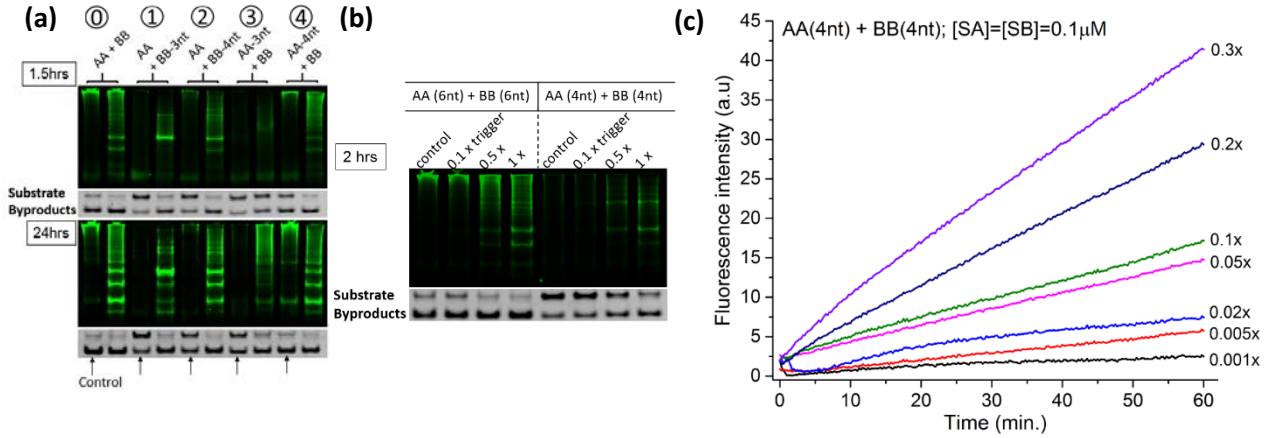

Figure S6. Characterizations of downstream subsystem with shortened assistant strands. (a) PAGE (8% gel) analysis examined the effects of shortened toeholds in assistant strands on downstream dendrimer self-assembly. Four distinct groups were tested (groups ①, ②, ③, ④) and compared to our original design (group ⓪). 'AA-3nt' means the toehold of AA strand was shortened to 3nt. Each group consisted of a control experiment (marked with arrow) and a positive experiment (the lane next to control). [SA] = [SB] = 0.15μM, [O] = [SA] for positive experiments. Both 1.5hrs and 24hrs timescale were applied to the experiments and compared in the gel. (b) PAGE (8% gel) analysis compared the downstream self-assembly performance of both AA and BB with 4nt toeholds length to the original design for 2hrs assay time, i.e. both AA and BB with 6nt toeholds length. Different amounts of O strands were added. [SA] = [SB] = 0.15μM, 0.1xtrigger means the concentration of O is 0.1 times the concentration of SA. (c) Downstream kinetics of shortened AA and BB strands with 4nt toeholds. A broad range of O strand concentrations were added. 0.001x trigger means the concentration of O is 0.001 times that of SA. Since the lowest target concentration tested is 0.001x (0.1nM), the end-point signal of 0.001x data was set as 100n.u. and other traces were normalized accordingly. Note that only the fluorescence signal after subtraction of the control signal is presented.

Section 4. Fold amplification comparison of upstream, downstream and integrated amplifiers.

Triplicate experiments were conducted for each scenario. The maximum obtainable concentration of fluorescent product was calculated based on the substrate concentrations, e.g., for upstream circuitry, 300 nM [S] was added, thus the maximum obtainable concentration of fluorescent product (R-O complex) should be 300 nM with completion of the substrate conversion. Similarly, 150 nM substrate A (SA) and 150 nM substrate B (SB) were provided in the downstream and integrated system, since both SA and SB possess one fluorophore, the maximum obtainable concentration of fluorescent product ($(FA\text{-}FB)_n$ complex) should also be 300 nM (mass conservation). The fold amplification was calculated as:

$$Fold\ amplification = \frac{F - Fb}{Fs - Fb} * \frac{[P]}{[I]}$$

Where F is the input-dependent observed fluorescent signal, F_b is the background signal (control signal, due to leakage issue), and F_s is the observed saturated fluorescent signal with complete substrate conversion.

In each scenario, 5 nM target was added as positive control, and 300 nM target was added for indicating saturation signal level. As shown in Fig.S7 (b) and (d), the fluorescent signal observed was nearly the same with either 300 nM input, 1μM input or direct addition of fluorophore attached ssDNA (FA, FB, both with 150 nM), further confirmed the downstream saturated fluorescent value (F_s) with complete reactant conversion. It is noted that the F_s for both downstream and integrated circuitry reached similar values in 1 hour reaction (Fig. S7 (b) and (c)) given the same substrate SA and SB concentrations, revealing the efficient coupling of our integrated networks and the effective conversion of upstream S to enabling O strand. The F_s values for upstream only circuit and downstream/integrated system are different because of the distinct fluorophore/quencher pairs used (Alex647 fluorophore for upstream reporter, FAM fluorophore for downstream substrates). The Fig.S7 (b) also shows the origin of downstream leakage. As limited fluorescent signals were observed when only SA + AA, SB + BB, or SA +SB exist in the solution, the leakage signal detected was barely due to imperfect annealing process (low signal with SA + SB), whereas mainly originated from the aberrant interactions between the assistant strands (AA and BB) and substrate SA and SB strands (high signal with SA + SB + AA + BB).

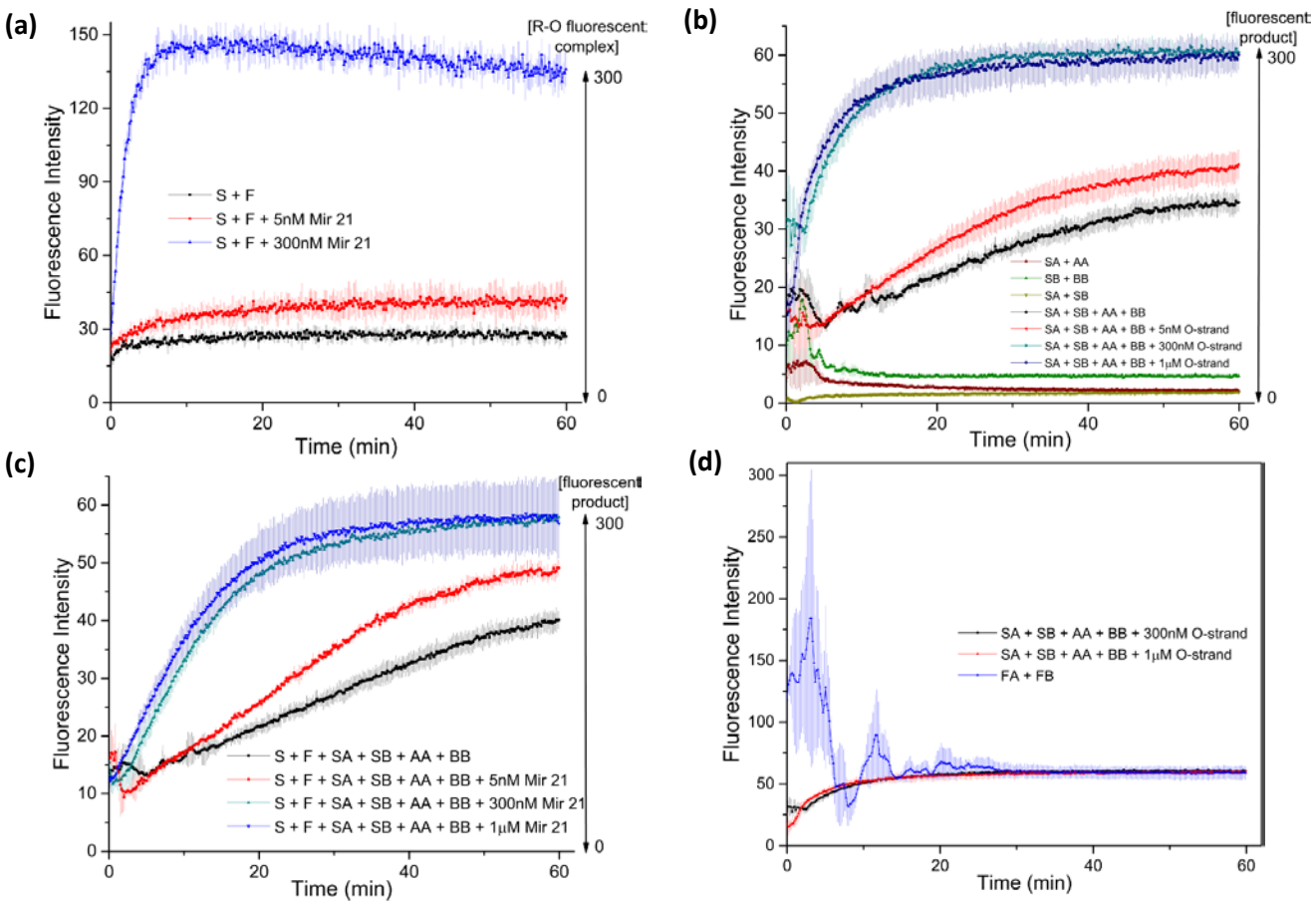

Figure S7. (a) Real-time fluorescence measurement of upstream only circuit, [S] = 300 nM, [F] = 600 nM, [R] = 900 nM, Mir 21 analog is the input molecule; (b) Downstream only circuit, [SA] = 150 nM, [SB] = 150 nM; O strand is the input molecule; (c) Integrated circuit, [S] = 300 nM, [F] = 600 nM, [SA] = 150 nM, [SB] = 150 nM; Mir 21 is the input molecule; (d) Saturation level of downstream circuit, [SA] = 150 nM, [SB] = 150 nM; [FA] = 150 nM, [FB] = 150 nM. All the experiments were conducted in the plate reader at 25°C incubation. The error bar indicates the standard derivation of each triplicate measurements.

References:

1. J. N. Zadeh, C. D. Steenberg, J. S. Bois, B. R. Wolfe, M. B. Pierce, A. R. Khan, R. M. Dirks and N. A. Pierce, *Journal of computational chemistry*, 2011, **32**, 170-173.
2. R. M. Dirks, J. S. Bois, J. M. Schaeffer, E. Winfree and N. A. Pierce, *SIAM review*, 2007, **49**, 65-88.
3. R. M. Dirks and N. A. Pierce, *Journal of computational chemistry*, 2004, **25**, 1295-1304.
4. Y. Gao, L. K. Wolf and R. M. Georgiadis, *Nucleic acids research*, 2006, **34**, 3370-3377.
5. D. Jose, K. Datta, N. P. Johnson and P. H. von Hippel, *Proceedings of the National Academy of Sciences*, 2009, **106**, 4231-4236.
6. R. M. Dirks and N. A. Pierce, *Proceedings of the National Academy of Sciences of the United States of America*, 2004, **101**, 15275-15278.
7. P. Yin, H. M. T. Choi, C. R. Calvert and N. A. Pierce, *Nature*, 2008, **451**, 318-322.
8. D. Y. Zhang and E. Winfree, *Nucleic acids research*, 2010, **38**, 4182-4197.
9. Y. S. Jiang, S. Bhadra, B. Li and A. D. Ellington, *Angewandte Chemie*, 2014, **126**, 1876-1879.
10. R. R. Machinek, T. E. Ouldridge, N. E. Haley, J. Bath and A. J. Turberfield, *Nature communications*, 2014, **5**.
11. A. J. Genot, D. Y. Zhang, J. Bath and A. J. Turberfield, *Journal of the American Chemical Society*, 2011, **133**, 2177-2182.
12. R. Deng, L. Tang, Q. Tian, Y. Wang, L. Lin and J. Li, *Angewandte Chemie International Edition*, 2014, **53**, 2389-2393.